Parametric dependence of beam-ion-driven modes in NSTX and NSTX-U

E. D. Fredrickson, R. Bell, A. Diallo, B. LeBlanc, F. Levinton[a], M. Podestá, H. Yuh[a]

Princeton Plasma Physics Laboratory, Princeton New Jersey 08543
[a]*Nova Photonics, Princeton, NJ 08543*

This paper presents an empirical approach towards characterizing the stability boundaries for some of the common energetic-ion-driven instabilities seen on the National Spherical Torus Experiment (NSTX/NSTX-U). Understanding the conditions for which beam-driven instabilities arise, and the extent of the resulting perturbation to the fast-ion population, is important for predicting and eventually demonstrating non-inductive current ramp-up and sustainment in NSTX-U, as well as the performance of future fusion plasma experiments such as ITER. In previous work [1], a database was constructed based on shots from the 2010 experimental campaign for which TRANSP runs were performed. Each shot was divided into 50 ms intervals and the dominant beam-driven activity was characterized, and plasma parameters were collected into a database. The parameter $<\beta_{fast}>/<\beta_{total}>$ was found to be useful for predicting where TAE avalanches and quiescent plasmas were found (Fig. 1).

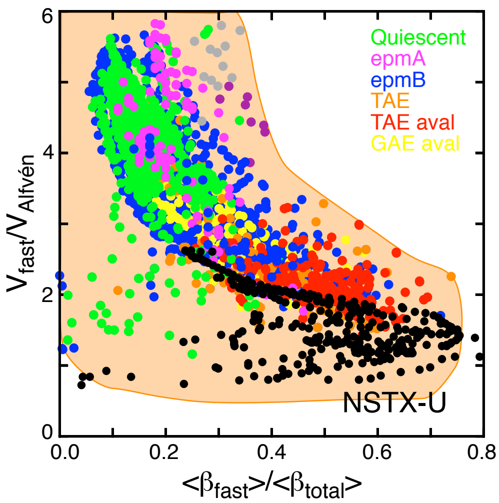

Fig. 1. The colored points are data from NSTX for a variety of fast-ion instabilities, the tan region corresponds to the approximate parameter range expected for NSTX-U. The black points are from initial NSTX_U shots.

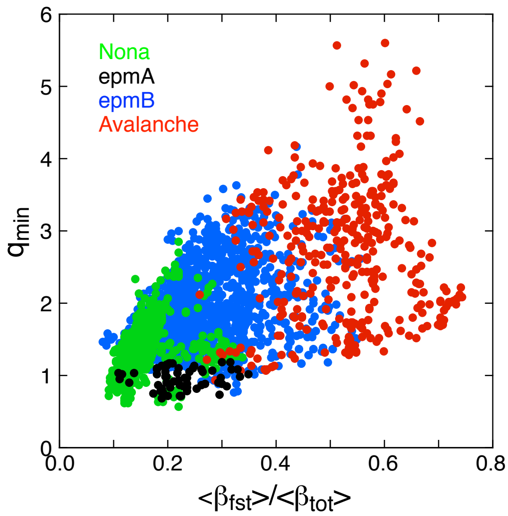

Fig. 2. Database showing existence of TAE avalanches (red), epmB (blue), epmA (black) and quiescent plasmas.

For this NSTX data set, the parameter $V_{fast}/V_{Alfvén} > 1$ due to the relatively low toroidal field. In future experiments, it is expected that the higher field of NSTX-U will extend the parameter $V_{fast}/V_{Alfvén}$ to significantly less than one. In fact, such plasmas have been generated, albeit with limited diagnostic coverage as yet. The black points (Fig 1) are from early NSTX-U shots at 6.5 kG. Ultimately, NSTX-U should operate with toroidal field up to 10 kG illustrated by the tan region in Fig. 1.

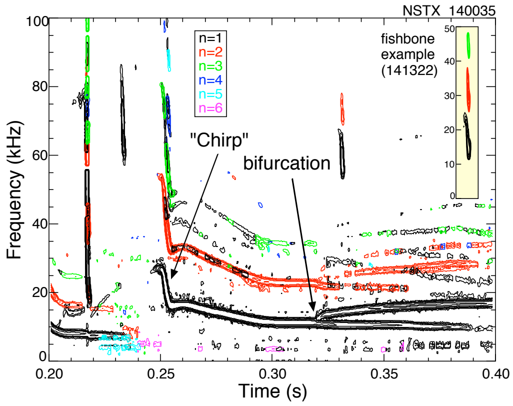

Fig. 3. Spectrogram showing onset of epmB with "chirp", followed by bifurcation at 0.32s. Inset shows fishbone mode for comparison.

The NSTX database has been extended to include q-profile and rotation profile information, which could be important for predicting stability of various modes. In the previous work, four types of modes were studied, Global Alfvén Eigenmodes (GAE), Toroidal Alfvén Eigenmodes (TAE), and two low frequency modes, a fishbone-like mode (epmA) and the epmB, a mode similar to the 'long-lived mode' [2]. In Fig. 2 is shown an existence plot for these modes in the space of q_{min} vs $\langle\beta_{fast}\rangle/\langle\beta_{total}\rangle$. In this dataset the fishbone-like modes (black dots) are found with $q_{min} \approx 1$, and for relatively low $\langle\beta_{fast}\rangle/\langle\beta_{total}\rangle$. Quiescent plasmas (not counting GAE or CAE activity) are found when $\langle\beta_{fast}\rangle/\langle\beta_{total}\rangle < 0.3$ and for $1 \leq q_{min} \leq 3$. So far, no correlation of the rotational shear has been found with mode stability, however, the rotation profile has been used to map the radial location of some modes.

At the onset of the epmB, the frequency chirps downward (Fig. 3) and the core rotation profile collapses (Fig. 4). as was reported on MAST. The range of the frequency chirp at the onset of long-lived modes is found to be consistent with the frequency change of the on-axis rotation, but the frequency drop off-axis is less, thus some of the frequency chirp may be due to fast particle effects. Occasionally, some 10's of msec later, but not always, the mode bifurcates into a low and high frequency branch. This bifurcation is accompanied by a re-peaking of the core rotation, presumably as the rotation sheared

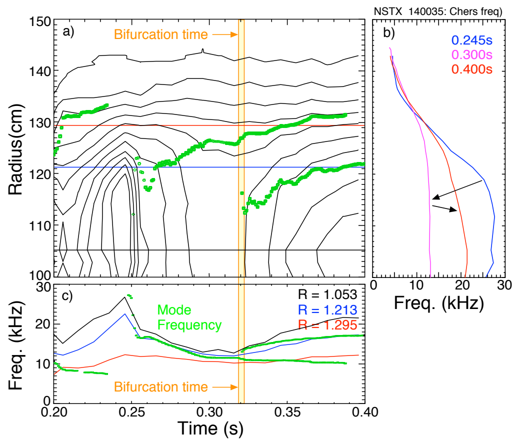

Fig. 4. a) Contours of the toroidal rotation profile showing effect of mode in Fig. 3 on core rotation. Green lines show where mode frequency matches plasma rotation. b) profiles of rotation from before collapse, during core flattened period and after recovery, c) rotation at the three radii indicated in a).

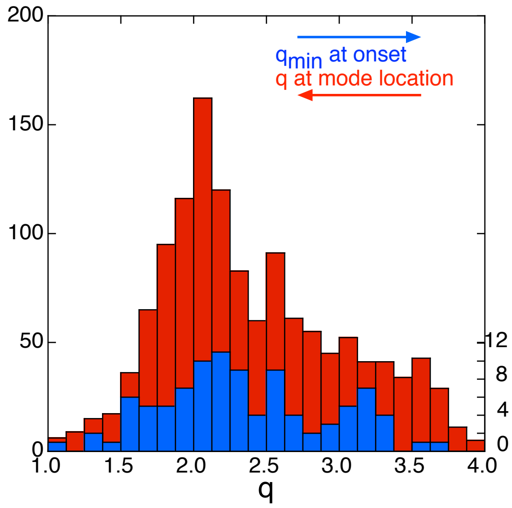

Fig. 5. Histograms of qmin at mode onset (blue) and q at the radius where plasma toroidal rotation matched the mode frequency.

the kink into two separate modes, one localized in the core region, the other farther out.

The onset of the epmB is only weakly correlated with q_{min} passing through a low-order rational surface. In Fig. 5 is shown a histogram of q_{min}'s at the onset of epmB's in this dataset (blue). There is a weak peaking around $q_{min} \approx 2.2$ and 3.3 as might be expected for infernal modes, but the correlation with low-order rational surfaces is not strong. The mode frequency evolution was tracked at 10 ms intervals, and the mode frequency was mapped to the plasma rotation, and then to the local q. That data is shown as the red histogram in Fig. 5. Now, the correlation with the q=2 rational surface is stronger, but the distribution is still quite broad. The weak peaks near q=2.5, q=3 and q=3.5 are probably not statistically significant. A strong correlation would be expected if a 2/1 island had formed, which would tend to lock the mode to the plasma rotation at the island rational surface.

Something resembling the opposite of this bifurcation has also been seen, but the cause may be different. In Fig. 6 is shown a spectrogram showing the onset of a similar low-frequency mode. The spectrum could be interpreted as multiple n=1 modes at different frequencies, coalescing to one mode at about 0.69s, however it seems unlikely that that many different modes would simultaneously become unstable. The amplitude envelope of all of the modes is modulated, similar to the case for the 'pitchfork modes' [3]. This might support a contention that fast-ions provided some of the drive for these modes. Note that the dominant n=2 (red) mode is not at twice the

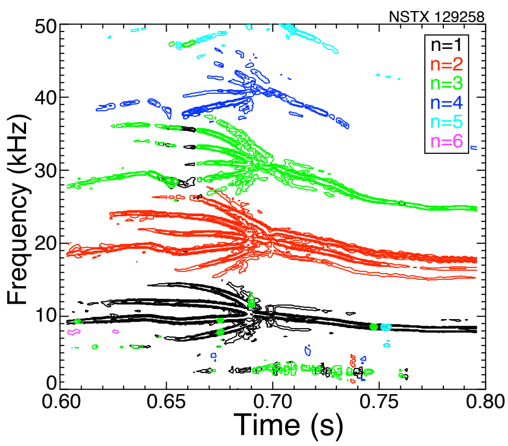

Fig. 6. Spectrogram showing onset of kink-like mode showing what appears to be a coalescence of multiple modes. It is unclear whether the higher n modes are independent of the n=1 kink mode.

n=1 frequency, thus is probably a mostly independent mode.

NSTX-U has three additional co-tangential neutral beam sources with tangency radii of 110cm, 120cm and 130cm (the magnetic axis is typically around R=100cm), so these sources deposit fast ions off of the magnetic axis. This suggests a further expansion of the dataset to include some information on the fast ion distribution function. Preliminary results from NSTX-U have already demonstrated that the shape of the fast-ion distribution function can be critically important for fast-ion driven mode stability.

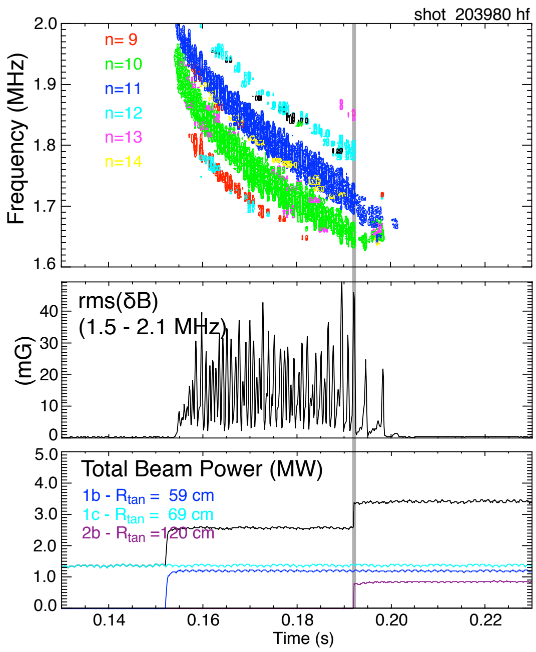

Fig. 7. a) color-coded spectrogram showing GAE activity. Dominant modes are n=9, red, n=10, green and n=11, blue. b) RMS magnetic fluctuation amplitude over the frequency range 1.5-2.1 MHz, c) total injected beam power, black curve, and injected power for each of the individual sources, magenta curve is off-axis.

Injection of one off-axis source is routinely seen to suppress multiple GAE excited by the sources injected inboard of the magnetic axis. TRANSP calculations of the fast-ion distribution function find that the injection of outboard beam sources fill in the distribution function in the region between roughly $0.8 < V_{||}/V < 1$, the inboard sources, injected more perpendicular, have larger $V_{\perp}/V$. The theory of GAE stability predicts drive and damping from fast ions as a function of the dimensionless parameter $k_{\perp}\rho$ [4], where ρ is the Larmor radius of the resonant energetic fast ion. The model predicts that for $k_{\perp}\rho < 1.9$, the resonant fast ions will be stabilizing, and destabilizing for $1.9 < k_{\perp}\rho < 3.9$. There is no experimental measurement of $k_{\perp}$, but this stability boundary is roughly consistent with estimates based on a simple dispersion relation and the resonance constraint for beam-driven GAE. The GAE may be stabilized by a change in the local gradients of the distribution function.

Work supported by U.S. DOE Contracts DE-AC02-76CH03073.

[1] E D Fredrickson, N N Gorelenkov, et al., Nucl. Fusion 54 (2014) 093007.
[2] I T Chapman, M-D Hua, S D Pinches, et al. Nucl. Fusion 50 (2010) 045007
[3] A Fasoli, B N Breizman, D Borba, et al., PRL 81 (1998) 5564.
[4] N N Gorelenkov, E Fredrickson, E Belova, et al. Nucl. Fusion 43 (2003) 228.